




# Reaction-Diffusion Equation with Stationary Wave Perturbation in Weakly Ionized Plasmas

S. T. da Silva<sup>1</sup> · R. L. Viana<sup>1</sup> 

Received: 14 July 2020 / Published online: 1 October 2020  
© Sociedade Brasileira de Física 2020

## Abstract

The influence of external harmonic forcing in nonlinear chaotic systems is a subject of active investigation, chiefly in low-dimensional dynamical systems, but fewer results are available for high-dimensional systems like plasmas. In this paper, we consider a theoretical model for a weakly ionized plasma, in which the following effects are taken into account: (i) ambipolar diffusion; (ii) the inflow of plasma particles through ionization processes; (iii) the outflow of plasma particles due to recombination. The spatiotemporal patterns of the resulting nonlinear system, as revealed by numerical integration of the reaction-diffusion partial differential equations, can be partially or totally suppressed through the action of acoustic waves forming stationary patterns in the plasma container. These suppression effects are quantitatively investigated by a number of numerical diagnostics like the average Lyapunov exponents and spatial correlation function. Suppression of spatiotemporal chaos can be achieved through adequate choices of amplitude and frequency of the applied waves.

**Keywords** Nonlinear reaction-diffusion equations · Weakly ionized plasmas · Fisher-KPP equation · Spatiotemporal chaos

## 1 Introduction

Chaos and turbulence are often seen as a great challenge in many situations of plasma physics interest [1, 2]. In fusion plasma physics, the existence of chaotic behavior often leads to turbulence [3, 4]. The combination of nonlinearity with other instability phenomena is a severe problem in the magnetic confinement of plasmas in fusion devices [2]. Generally, one has to distinguish between temporal low-dimensional chaos, related to oscillations, and spatiotemporal chaos, related to waves, also classified as weakly developed turbulence [5].

In the framework of nonlinear dynamical systems, several strategies have been developed to obtain active control over complex temporal or spatiotemporal behavior [5, 6]. Recent applications of control theory have been developed to control chaotic behavior [7, 8]. For example, small perturbations have been used to control chaotic oscillations of the current and plasma potential in plasma diodes [9].

Successful approaches in controlling chaos in low-dimensional systems have motivated the search of techniques for taming fully developed spatiotemporal chaos. As an example, continuous global control can be used to stabilize plasma turbulence due to weakly developed ionization waves [9, 10].

A system that presents a rich dynamics with spatiotemporal chaos is the reaction-diffusion equation in weakly ionized plasmas [11]. Depending on the parameter values, such systems can display spatiotemporal chaos. Particularly in technological plasmas, it is of great interest to understand the physics of control or suppression of turbulence in this system [12]. The reaction-diffusion model used in this paper is characterized by the simultaneous presence of a diffusion and a nonlinear reaction term, where the diffusion term leads to configurations where density gradients are smoothed out [13].

Reaction processes, on the other hand, are nonlinear interaction processes like ionization and recombination, leading to positive and negative source terms. The competition of reaction and diffusion can lead to either simple, uniform, equilibrium configuration as well a complicated pattern formation, including the possibility of spatiotemporal chaos [14, 15]. The transition to spatiotemporal chaos in a weakly ionized magnetoplasma was experimentally investigated in

✉ R. L. Viana  
viana@fisica.ufpr.br

<sup>1</sup> Departament of Physics, Federal University of Paraná, Curitiba, Paraná, 81531-990, Brazil

a cylindrical RF magnetron, showing a substantial reduction of spatiotemporal coherence with large RF power [16].

One of the various spatiotemporal patterns that are possible in nonlinear reaction-diffusion systems is the creation of spatially localized regions of chaotic behavior [17, 18]. In a recent work, it has been shown that, depending on the parameters of the reaction and diffusion, the plasma can present regimes where it has turbulent regions mixed with periodic regions, to regimes where the plasma has fully developed turbulence [19]. A discrete version of this model, yielding a coupled map lattice, has also been investigated leading to qualitatively similar behavior [20]. The goal of the present work is to understand the spatiotemporal dynamics that occurs when we apply an external perturbation in the form of a standing wave.

In the present work, we show that the injection of external electrostatic waves, forming stationary wave patterns in the plasma container, can exhibit different effects, being able to suppress or mitigate the space-time chaos, as to trigger this effect. A tool used to quantify the influence of the disturbance on the turbulent plasma regime is called the average Lyapunov exponent, developed by Shibata [21, 22] for the temporal dynamics of a spatially extended system. Using the spatial correlation function, we characterize the spatial profiles with fixed time for different amplitudes of the applied external wave [23]. The spatial correlation function is very useful in the characterization of spatiotemporal chaos in a spatially extended system [24].

The rest of this article is organized as follows: in Section 2, we derive the reaction-diffusion equation with a sinusoidal external perturbation that describes a bounded one-dimensional weakly ionized plasma with applied density waves. In this section, we also present spatiotemporal patterns obtained through numerical integration of the equation for nonlinear reaction-diffusion perturbation, for limited parameter ranges of interest in plasma physics. Section 3 deals with the average Lyapunov exponents used to characterize the chaoticity of the spatiotemporal profiles and how they are affected by the external wave perturbation. The spatial correlation function for different spatiotemporal profiles is dealt with in Section 4. The last section contains our conclusions.

## 2 Reaction-Diffusion with Stationary Wave Perturbation

In this section, we outline the theoretical model used to derive the reaction-diffusion equation which describes a non-magnetized weakly ionized plasma. Assuming the existence of ambipolar diffusion, the nonlinear

reaction-diffusion equation for a weakly ionized plasma can be written in the form

$$\frac{\partial n(\mathbf{r}, t)}{\partial t} - D \nabla^2 n(\mathbf{r}, t) = Q(\mathbf{r}, t), \quad (1)$$

where  $n = n_e$  is the electron density of the plasma (equal to the ion density  $n_i$  due to quasi-neutrality),  $D > 0$  is a constant diffusion coefficient, and  $Q(\mathbf{r}, t)$  is a source term.

The source term has both positive and negative contributions, representing production and loss terms, respectively [25]. The positive source term is represented by ionization [11] which is proportional to the product between electron density  $n_e = n$  and neutral atom density  $n_a$

$$Q^+ = \left( \frac{\partial n}{\partial t} \right)_{ion} \equiv an, \quad (2)$$

where  $a > 0$  is the ionization coefficient. Another type of source is known as recombination [11], which corresponds to a sink that acts as a loss term. Recombination occurs when a negative ion captures a free electron, the recombination rate being proportional to the product between electron and ion densities:

$$Q^- = \left( \frac{\partial n}{\partial t} \right)_{rec} \equiv -bn^2, \quad (3)$$

where  $b > 0$  is the recombination coefficient. We thus have two kinds of reaction processes: ionization, which acts as a source, and recombination, which acts as a sink, the nonlinear reaction term being written as

$$Q(n) = Q^+ + Q^- = an - bn^2. \quad (4)$$

After substitution into (1), we have a nonlinear reaction-diffusion equation

$$\frac{\partial n}{\partial t} - D \nabla^2 n = n(a - bn). \quad (5)$$

Let us consider a one-dimensional version of the reaction-diffusion equation (5), where the plasma is confined by metallic (perfectly conducting) walls at  $x = 0$  and  $x = \ell$ , respectively, corresponding to the boundary conditions

$$n(x = 0, t) = n(x = \ell, t) = 0. \quad (6)$$

Moreover, we have to specify the initial condition, which is a given spatial pattern  $n(x, t = 0)$ .

If we neglect the diffusion coefficient in (5), the resulting differential equation has an elementary solution, namely

$$n(D = 0, t) = \frac{aC}{e^{-at} + bC}, \quad (7)$$

where the integration constant is expressed in terms of the initial condition  $n(t = 0)$

$$C = \frac{n(t=0)}{a - bn(t=0)}, \quad (8)$$

and such that, if  $a > 0$ , for large times the density tends to the stationary value  $n_0 = a/b$ .

Considering also a characteristic time  $t_0$ , we can define normalized variables as  $u = n/n_0$ ,  $\rho = x/\ell$ ,  $\tau = t/t_0$ , in such a way that the reaction-diffusion equation now reads

$$\frac{\partial u}{\partial \tau} - \varepsilon \frac{\partial^2 u}{\partial \rho^2} = \alpha u(1 - u), \quad (9)$$

where the number of system parameters has been reduced from three to just two, namely

$$\varepsilon \equiv \frac{Dt_0}{\ell^2}, \quad \alpha \equiv at_0, \quad (10)$$

representing the coupling constant due to diffusion and the overall nonlinearity parameter due to reaction processes, respectively. The expression (9) is the so-called Fisher-KPP equation, with many physical and biological applications [19].

We model the influence of an external density disturbance on a non-magnetized weakly ionized plasma, and we consider an ion-acoustic wave injected into the plasma. Due to the bounding metallic walls, after a short time, we expect the presence of stationary wave patterns. For simplicity, we consider a single resonant mode, with nodes at the walls ( $\rho = 0$  and  $\rho = 1$ ) and at the center point  $\rho = 0.5$ . This

adds a new term on the right side of the reaction-diffusion equation (9) such that it can be written in the form:

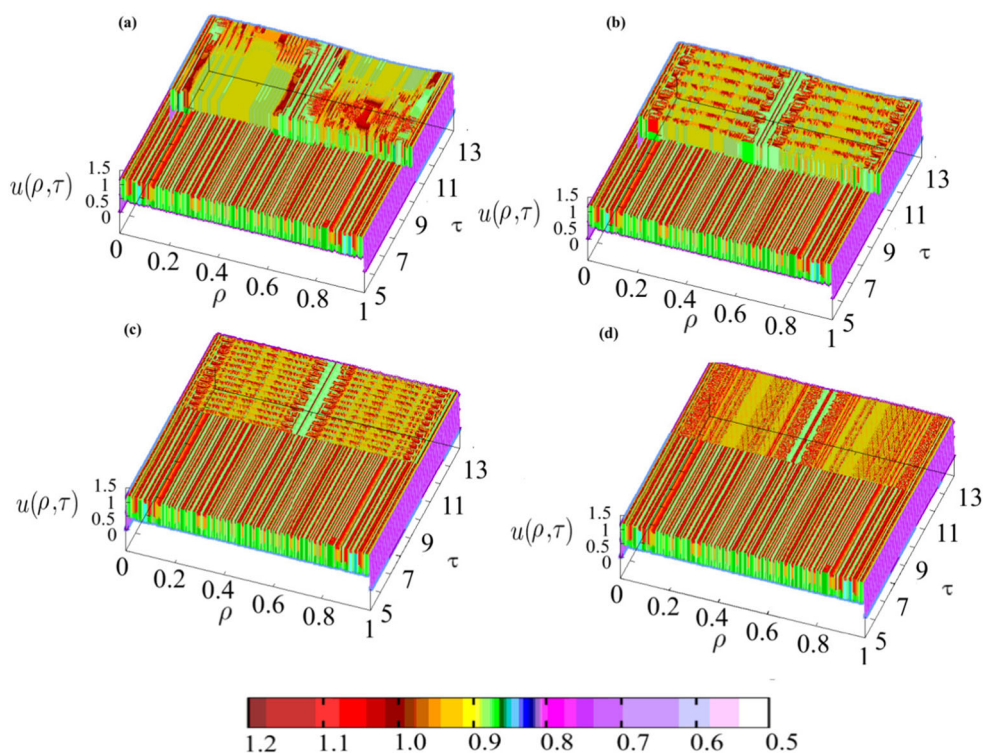
$$\frac{\partial u}{\partial \tau} - \varepsilon \frac{\partial^2 u}{\partial \rho^2} = \alpha u(1 - u) + u_0 \sin(2\pi\rho) \sin(\omega\tau), \quad (11)$$

where  $u_0$  and  $\omega$  are the amplitude and frequency of the stationary wave, respectively.

The resulting partial differential equation with external perturbation given by (11) was solved, with boundary conditions (6) using an implicit finite difference scheme. The time and space steps used in the integration were chosen as  $\Delta\tau = 10^{-4}$  and  $\Delta\rho = 5 \times 10^{-3}$ , respectively. The initial profile was specified as  $u(\rho, 0) = \sin(2\pi\rho)$ . Since the system is globally dissipative, and we have discarded a large number of transient times, the spatial patterns observed were found not to depend on the initial conditions used. On the other hand, the fixed boundary conditions used in our numerical simulations affect in a very important way the spatiotemporal dynamics.

Initially we show numerical results illustrating the effect of waves of different frequencies on a plasma with spatiotemporal chaotic dynamics (a regime called *frozen random pattern*, [19]), that can be found for a coupling coefficient  $\varepsilon = 0.01$ , and a nonlinearity parameter  $\alpha = 2.6 \times 10^4$ , for example. The frozen random pattern has, as main characteristics, a large number of small domains with low temporal periods mixed with equally small regions with chaotic motion. These patterns are “frozen” in the sense that their boundaries do not move with time. Figure 1a–d are

**Fig. 1** Space-time plots of the normalized plasma density (in colorscale) for  $\varepsilon = 0.01$ ,  $\alpha = 2.60 \times 10^4$ , where an external wave perturbation of amplitude  $u_0 = 0.04$  is applied at  $\tau = 10$  with different frequencies:  $\omega =$  (a) 1, (b) 10, (c) 20, and (d) 100



space-time plots of the normalized density before and after the application (at time  $\tau = 10$ ) of a stationary wave of fixed amplitude  $u_0 = 0.04$  and different frequencies  $\omega$ .

For all cases depicted in Fig. 1, we observe a breakdown of the frozen random patterns after the wave is switched on, and the plasma is forced to oscillate at the same spatial mode as the external wave, with a node at the center point  $\rho = 0.5$ . For small frequency, the patterns are almost as irregular as before (Fig. 1a) but, as  $\omega$  increases, the plasma density exhibits oscillations with roughly the same frequency as the external wave, in an example of entrainment (Fig. 1b–d).

Another example of the effect of an external stationary wave is illustrated in Fig. 2, where we have a spatiotemporal pattern with chaotic defects, before the perturbation is switched on. Chaotic defects are spatially localized chaotic regions and bounded by regions of low temporal periods known as *zigzag* domains. These defects move along the lattice in a Brownian motion with memory [19, 20].

After the application of the stationary wave at  $\tau = 10$ , with low frequency, we observe that the chaotic defect does not disappear but is spatially displaced or reappears after a transient (Fig. 2a). For higher frequencies, however, the chaotic defects disappear and are replaced by oscillations nearly resonant with the external forcing (Fig. 2b–d).

A third example is provided by Fig. 3a–d, where the dynamical regime before the perturbation is switched on can be classified as spatiotemporal intermittency pattern, for which there is an intermittent transition between chaotic and

regular oscillations. After the perturbing wave is applied, the plasma response follows the same spatial pattern of the wave, with oscillations entrained to the external perturbation. Moreover, we observe an overall decrease in the turbulent density oscillations, since the density tends to concentrate on the wave maxima.

### 3 Average Lyapunov Exponent

Some of the conclusions we obtained in the previous section were essentially qualitative and based on a superficial inspection of the space-time plots. A proper characterization of the degree of suppression of chaotic behavior, in both space and time, would need suitable numerical diagnostics.

One of these diagnostics is the average Lyapunov spectrum for the partial differential equation (11), obtained through the application of a method proposed by Shibata [21, 22]. From the numerical integration scheme, we transform (11) into a finite difference equation in the form

$$\frac{u_j^{k+1} - u_j^k}{\Delta\tau} = h(\Delta\rho, \{u_j^k\}), \quad (12)$$

where  $\Delta\tau$  and  $\Delta\rho$  are the time and space steps, respectively, and  $(k, j)$  denote the discrete time and position, such that  $u_j^k = u(\rho = j\Delta\rho, \tau = k\Delta\tau)$ , where  $k, j = 1, 2, \dots, N -$

**Fig. 2** Space-time plots of the normalized plasma density (in colorscale) for  $\varepsilon = 0.01$ ,  $\alpha = 2.8202 \times 10^4$ , where an external wave perturbation of amplitude  $u_0 = 0.04$  is applied at  $\tau = 10$  with different frequencies:  $\omega =$  (a) 1, (b) 10, (c) 20, and (d) 100

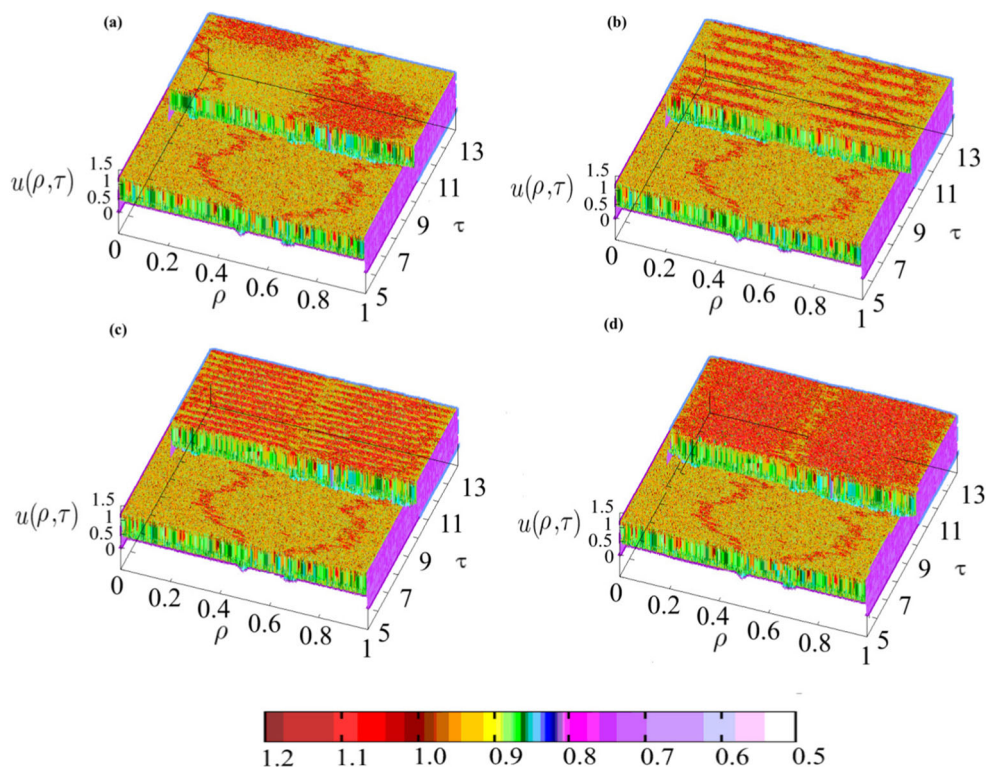
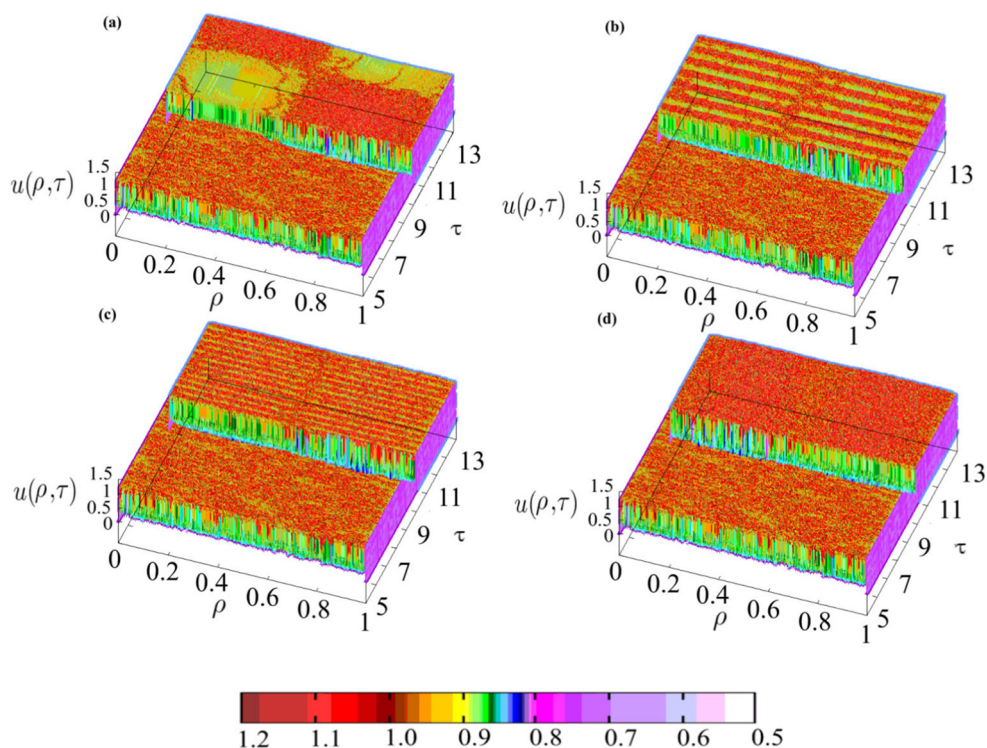


**Fig. 3** Space-time plots of the normalized plasma density (in colorscale) for  $\varepsilon = 0.01$ ,  $\alpha = 2.83 \times 10^4$ , where an external wave perturbation of amplitude  $u_0 = 0.04$  is applied at  $\tau = 10$  with different frequencies:  $\omega =$  (a) 1, (b) 10, (c) 20, and (d) 100



1. The corresponding Jacobian matrix at time  $k\Delta\tau$  has elements

$$B_{ij}^{k,N} = \frac{\partial u_i^{k+1}}{\partial u_j^k}, \quad (i, j = 1, 2, \dots, N-1). \quad (13)$$

According to Shibata, the average Lyapunov exponent at discrete time  $k$  is defined by

$$\lambda_k = \frac{1}{N} \ln |\det B^{k,N}|. \quad (14)$$

The reasoning behind this definition is that the determinant of the Jacobian matrix (13) can be interpreted as representing the disorderness of the state variable  $u$  at discrete time  $k$  [22]. Hence, the average Lyapunov exponent (14) represents the mean degree of this disorderness over the lattice, yielding a larger value when the spatial disorder is higher. However, as the dynamical system evolves with time, the degree of disorderness represented by  $\lambda_k$  varies with time, in such a way that it is better to work with the temporal mean of the average Lyapunov exponent

$$\Lambda = \frac{1}{n_k} \sum_{k=1}^{n_k-1} \lambda_k, \quad (15)$$

where  $n_k$  is a large integer, chosen after transients have decayed.

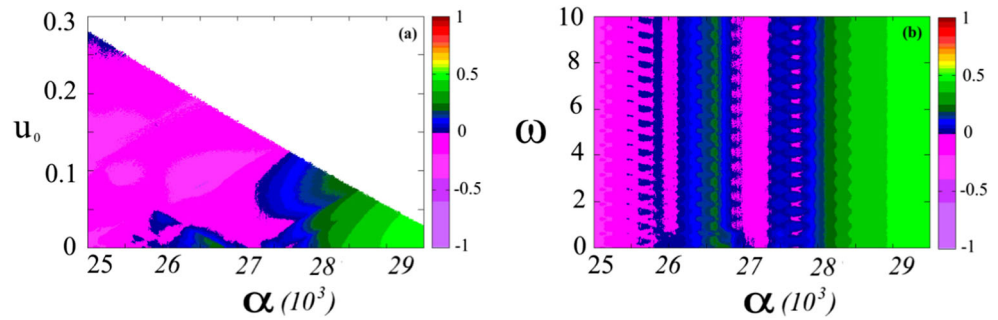
It must be emphasized that these averaged Lyapunov exponents are different from those usually computed in phase space, and which measure the exponential rate of separation between two initially close trajectories. As

defined by Shibata, the average exponent must be taken as a local measure of disorder, and do not correspond to exponential separation rates. However, the general interpretation is basically the same: positive values of  $\Lambda$  indicate spatial disorder, whereas negative values are related to ordered patterns.

We plot in Fig. 4a–b the values of  $\Lambda$  (in colorscale) as a function of different pairs of parameters. The regions for which the exponent diverges to minus infinity are painted white. In the absence of external perturbation ( $u_0 = 0$ ), the exponent varies from negative to positive according to the degree of disorder (i.e., increasing  $\alpha$ ). In fact, the examples depicted in Figs. 1, 2, and 3 correspond to different regions of spatiotemporal behavior along this line: frozen random patterns, chaotic defects, and spatiotemporal intermittency, with an increasing degree of disorder.

As the perturbation is switched on, we have substantial modifications in this profile. As  $u_0$  increases, the value of  $\Lambda$  achieves minus infinity (white regions in Fig. 4a) indicating that the wave perturbation has been able to effectively suppress the spatiotemporal chaos, yielding more ordered patterns. In fact, Figs. 1, 2, and 3 show that the spatiotemporal patterns become entrained with the external perturbation, oscillating with the wave frequency. It is worth noting that the critical values of  $u_0$ , above which the value of  $\Lambda$  goes to minus infinity, lay on a straight line with negative slope. In Fig. 4b, the value of  $\Lambda$  is plotted against the wave frequency  $\omega$  and the nonlinearity  $\alpha$ . Here we observe that the effect of increasing frequency is only noticeable for

**Fig. 4** Average Lyapunov exponent (in colorscale) as a function of the pair of parameters: **(a)** wave amplitude  $u_0$  and nonlinearity  $\alpha$  for fixed wave frequency  $\omega = 10$ ; **(b)** wave frequency  $\omega$  and nonlinearity  $\alpha$  for fixed wave amplitude  $u_0 = 0.04$



small values of  $\omega$ , a fact already seen in the space-time plots of Figs. 1, 2, and 3.

The effect of different wave amplitudes and frequencies for increasing nonlinearity can be also seen in Fig. 5, where we plot the average Lyapunov exponent  $\Lambda$  as a function of the wave frequency  $\omega$  for three different amplitudes  $u_0 = 0.02, 0.04$ , and  $0.08$ ; and different values of the nonlinearity parameter. In Fig. 5a obtained for  $\alpha = 2.60 \times 10^4$  and  $\varepsilon = 0.01$  (for which the unforced system displays frozen random patterns), we see  $\Lambda$  is practically independent on the wave frequency, but there is a decrease of the average Lyapunov exponent as we increase the amplitude of the perturbation. In other words, there is a decrease in the of spatiotemporal chaos in the plasma, as we switch on the wave perturbation.

Figure 5b, for  $\alpha = 2.8205 \times 10^4$  and  $\varepsilon = 0.01$ , which shows chaotic defects in the absence of wave perturbation, displays an increase of  $\Lambda$  with  $\omega$ , and a decrease of  $\Lambda$  with  $u_0$ , as in the previous case. Hence, the effect of wave frequency is more pronounced on the dynamics of chaotic defects. The same features are shown in Fig. 5c for  $\alpha = 2.8300 \times 10^4$  and  $\varepsilon = 0.01$  (the unperturbed system exhibits spatiotemporal intermittency).

## 4 Spatial Correlation Function

Another quantitative index that we can use to characterize spatiotemporal patterns and the influence of the wave

perturbation is the so-called spatial correlation function, which has been used to investigate many dynamical effects in spatially extended systems. For a fixed time  $\tau = k\Delta\tau$ , the spatial average of the normalized density for the system is

$$\langle u \rangle(\tau) = \frac{1}{N} \sum_{j=1}^N u(\rho = j\Delta\rho, \tau), \quad (16)$$

and the corresponding deviation from this average is

$$\hat{u}(\rho = i\Delta\rho, \tau) = u(\rho = i\Delta\rho, \tau) - \langle u \rangle(\tau). \quad (17)$$

We define the spatial correlation function, which characterizes the correlation between the different individual lattice sites, as [24]

$$C(\rho = j\Delta\rho, \tau) = \frac{\sum_{i=1}^N \hat{u}(\rho = i\Delta\rho, \tau) \hat{u}(\rho = (i+j)\Delta\rho, \tau)}{\sum_{i=1}^N \{\hat{u}(\rho = i\Delta\rho, \tau)\}^2} \quad (18)$$

The definition above is similar to the time correlation function of a time series, the difference is that we consider spatial averages instead of time averages, and the values considered in (18) are taken at a fixed time.

We show in Fig. 6 the dependence of the spatial correlation on the spatial separation  $j\Delta\rho$  along the lattice, for three different spatiotemporal profiles with and without perturbation. For all cases, we take a fixed time  $\tau = 10$ ,  $\varepsilon = 0.01$ ,  $\omega = 10$  and different values of  $\alpha$  and  $u_0$ . In

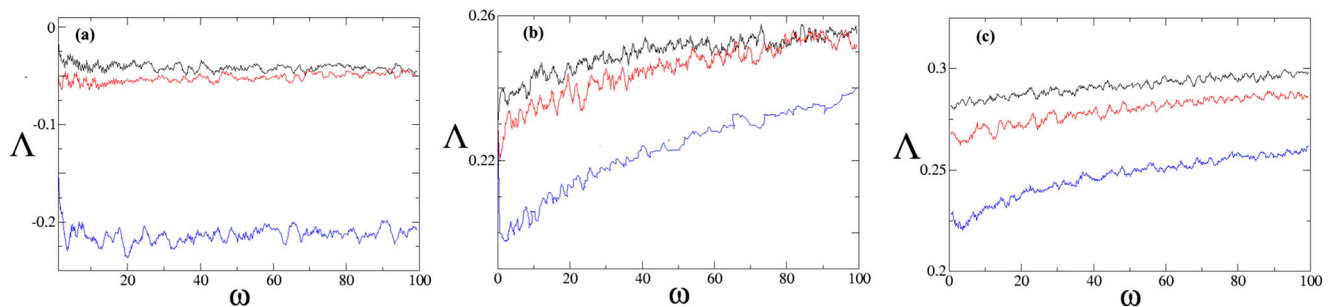


**Fig. 5** Average Lyapunov exponent  $\Lambda$  versus wave frequency  $\omega$  for  $u_0 = 0.02$  (black curves),  $u_0 = 0.04$  (red curves), and  $u_0 = 0.08$  (blue curves) for  $\varepsilon = 0.01$  and  $\alpha = 2.60 \times 10^4$  (a),  $2.8205 \times 10^4$  (b), and  $2.83 \times 10^4$  (c)

**Fig. 6** Spatial correlation function as a function of the lattice separation at a fixed time  $\tau = 10$ , for  $\varepsilon = 0.01$ ,  $\omega = 10$ , and: (a)  $\alpha = 2.60 \times 10^3$ , (b)  $2.70 \times 10^3$  and (c)  $2.82 \times 10^3$ . The wave amplitudes are  $u_0 = 0$  (red curve), 0.04 (blue curve), and 0.08 (green curve)

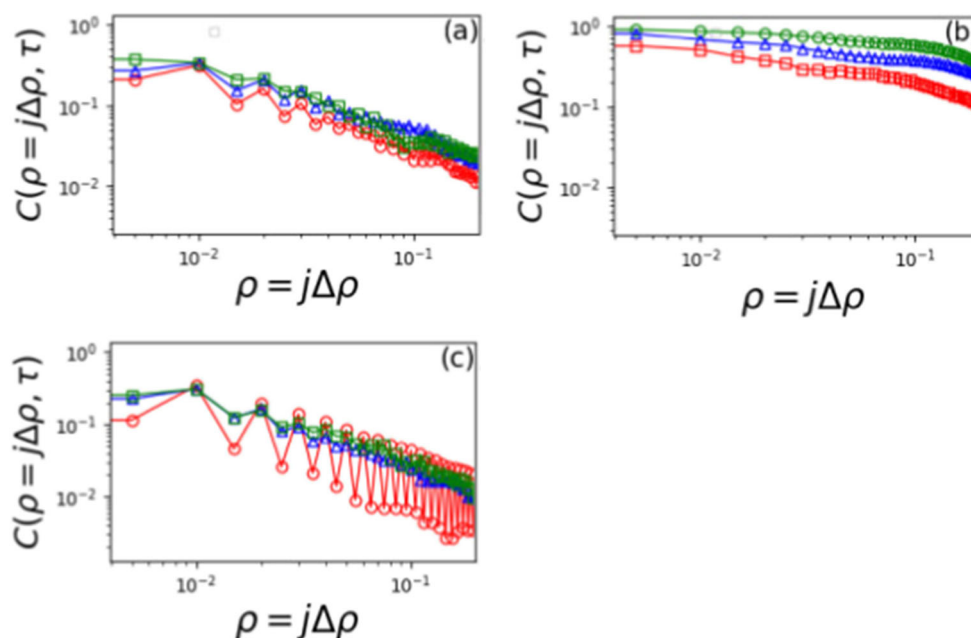


Fig. 6a, we consider  $\alpha = 2.60 \times 10^4$ , for which there is a frozen random pattern without perturbation (red curve). The data are well-adjusted by a power law in the form

$$C(\rho = j\Delta\rho, \tau) = C_0(j\Delta\rho)^{-\gamma} \quad (19)$$

where the decay exponent is  $\gamma = 0.0575$  (Table 1), with regression coefficient  $R^2 = 0.9294$ . The closer the latter is to the unity, the more representative the regression.

After the application of an external wave with amplitudes  $u_0 = 0.04$  (blue curve), the spatial correlation also decays as a power law with exponent 0.053, which is slightly less than for the unperturbed case. Increasing the wave amplitude to 0.08 (green curve), however, the decay exponent decreases to 0.039, indicating a slower decay and a diminishing

disorder in the spatiotemporal profile with respect to the amplitude of the applied wave.

The same observations can be made for the case depicted in Fig. 6b, where  $\alpha = 2.70 \times 10^4$ . The unperturbed case (red curve) corresponds to a pattern selection, and the power-law decay occurs with a smaller exponent, namely 0.046. The application of the external wave (blue and green curves) yields a slower power-law decay, also suggesting a decrease of the spatial disorder caused by the wave.

A similar behavior can also be identified in Fig. 6c, where  $\alpha = 2.82 \times 10^4$ , corresponding to chaotic defects when unperturbed. The novel feature here is that there is an oscillating behavior of the spatial correlation function for the unperturbed case. This can be due to the existence of zigzag patterns in both sides of a chaotic defect, as observed in coupled map lattices. The decay becomes more regular, however, as the wave perturbation is switched on, with a slightly smaller decay exponent reflecting a relatively mild effect of the external wave.

There are some arguments that can be used to justify the conclusions drawn upon the decay of the spatial correlation function. We start from the assumption that spatial correlations (at fixed time) are for spatial profiles as the time correlations (at fixed position) are for time series. The latter have been extensively studied in the context of nonlinear dynamics.

For hyperbolic chaotic systems, it is known that time-correlations decay exponentially in time [26]. For chaotic orbits of area-preserving non-hyperbolic systems, it has been shown that time correlations decay as a power law due to the presence of stickiness [27]. The latter is a kind of

**Table 1** Values of the coefficients of the power-law fitting (19) for the decay of the spatial correlation functions depicted in Fig. 6

$\alpha/10^4$	$u_0$	$C_0$	$\gamma$	$R^2$
2.60	0.00	1.057	0.0575	0.9294
2.60	0.04	1.053	0.0531	0.9542
2.60	0.08	1.042	0.0393	0.9623
2.70	0.00	1.653	0.0459	0.9346
2.70	0.04	1.271	0.0229	0.9531
2.70	0.08	1.095	0.0931	0.9345
2.82	0.00	1.047	0.0438	0.9294
2.82	0.04	1.044	0.0399	0.9532
2.82	0.08	1.034	0.0336	0.9492

behavior caused by stretches of almost-periodic behavior in a chaotic orbit near enough a periodic island [28].

Using the abovementioned analogy, if a spatial profile is highly disordered, it would be reasonable to speculate that spatial correlations also would decay exponentially. However, since the spatial disorder is not completely chaotic in spatiotemporal patterns, we expect a power-law decay of spatial correlations, which holds for the cases depicted in Fig. 6. From the analogy with the temporal case, the more spatially ORDERED is the pattern, the slower will BE the spatial correlation decay, and that is what we see after the application of the external wave.

## 5 Conclusions

Reaction-diffusion systems have many applications in fusion, astrophysical, and technological plasmas, and they provide simple yet efficient mathematical models for the description of many spatiotemporal phenomena. There is a rich variety of dynamic pattern formations depending on the parameters used, such as regimes containing chaotic and regular regions to regimes with fully developed space-time chaos, for example. We observed that the application of an external wave drives the plasma to oscillate at the same frequency as the applied wave. There is also a decrease in the space-time chaos, as we increase the amplitude of the applied wave, that is, the external wave acts to decrease these chaotic regions. These conclusions were obtained from an average Lyapunov exponent.

Another analysis that confirms this decrease in spatial disorder was performed using spatial correlation, where we observed a decrease in the correlation decay as a function of the wave amplitude. The cases we studied show a power-law decrease, what can be justified from an analogy with time correlations. The power-law decay becomes slower after the application of the wave perturbation, indicating a decrease of the spatial disorder.

One shortcoming of our theoretical model is that we considered just one species of particles in the plasma (free electrons) and is thus of limited application since we did not describe self-consistently the dynamics of the positive ions and neutral atoms. It is conceptually possible to extend the present analysis to a full description of diffusion-reaction involving also ions and neutral atoms. However, our aim was to show that even a toy model like the present one is able to describe the formation of complex spatiotemporal patterns, in particular those involving temporal chaos and spatial disorder. Moreover, the pure electron model can also explain

the decrease of spatial disorder through the application of stationary wave perturbations.

**Funding** This work has the partial financial support of CNPq (proc. 301019/2019-3).

## References

1. Y. Elskens, D. Escande, *Microscopic Dynamics of Plasmas and Chaos* (Institute of Physics Publishing, Bristol and Philadelphia, 2003)
2. W. Horton, Y.H. Ichikawa (eds.), *Chaos and Structures in Nonlinear Plasmas* (World Scientific, Singapore, 1996)
3. T.S. Hahmand, K.H. Burrell, *Phys. Plasmas* **2**, 1648 (1995)
4. G.D. Conway, *Plas. Phys. Contr. Fusion* **40**, 124026 (2008)
5. P. Manneville, *Dissipative Structures and Weak Turbulence* (Academic Press, San Diego, 1990)
6. H. Pécseli, *Fluctuations in Physical Systems* (Cambridge University Press, Cambridge, 2000)
7. T. Kapitaniak, *Controlling Chaos* (Academic Press, New York, 1996)
8. H.G. Schuster, *Handbook of Chaos Control* (Wiley-VCH, Weinheim, 1999)
9. T. Klinger, C. Schröder, D. Block, F. Greiner, A. Piel, G. Bonhomme, V. Naulin, *Phys. Plasmas* **8**, 1961 (2001)
10. C. Schröder, T. Klinger, D. Block, A. Piel, G. Bonhomme, V. Naulin, *Phys. Rev. Lett.* **86**, 25 (2001)
11. H. Wilhelmsson, E. Lazzaro, *Reaction-Diffusion Problems in the Physics of Hot Plasmas* (IOP Publishing, Bristol, 2001)
12. M.A. Lieberman, A.J. Lichtenberg, *Principles of Plasma Discharges and Materials Processing* (Wiley, New York, 2005)
13. W.B. Thompson, Introduction to kinetic theory of plasma. in *Physics of Hot Plasmas*, ed. by B.J. Rye, J.C. Taylor (Oliver and Boyd, Edinburgh, 1970)
14. P.O.J. Scherer, S.F. Fischer, *Reaction-Diffusion Systems*: Springer, Berlin-Heidelberg (2017)
15. I.R. Epstein, I.B. Berenstein, M. Dolnik, V.K. Vanac, L. Yang, A.M. Zhabotinsky, *Phil. Trans. R. Soc. A* **366**, 397 (2008)
16. J.H. Chu, I. Lin, *Phys. Rev. A* **39**, 233 (1989)
17. V.K. Vanag, I.R. Epstein, *Chaos* **17**, 037110 (2007)
18. K. Kaneko, *Physica D* **34**, 1 (1989)
19. S.T. da Silva, T. de L. Prado, I.L. Caldas, S.R. Lopes, R.L. Viana, *CNSNS*, submitted for publication
20. S.T. da Silva, T.L. Prado, S.R. Lopes, R.L. Viana, *Chaos* **071104**, 29 (2019)
21. H. Shibata, *Physica A* **264**, 226 (1999)
22. H. Shibata, *Physica A* **252**, 428 (1998)
23. J.M. Houlrik, M.H. Jensen, *Phys. Lett. A* **163**, 275 (1992)
24. D.B. Vasconcelos, R.L. Viana, S.R. Lopes, *Physica A* **343**, 201 (2004)
25. A. Fridman, L.A. Kennedy, *Plasma Physics and Engineering*, 2nd edn. (CRC Press, Boca Raton, 2011)
26. H. Fujisaka, T. Yamada, *Z. Naturforsch* **33(a)**, 1455 (1978)
27. C.F.F. Karney, *Physica D* **8**, 360 (1983)
28. G. Contopoulos, M. Harsoula, *Int. J. Bifurcat. Chaos* **18**, 2929–2949 (2008)

**Publisher's Note** Springer Nature remains neutral with regard to jurisdictional claims in published maps and institutional affiliations.